Published in final edited form as:
Nat Med. 2001 March ; 7(3): 331–337. doi:10.1038/85480.

Persistently modified h-channels after complex febrile seizures convert the seizure-induced enhancement of inhibition to hyperexcitability

Kang Chen[1,2], **Ildiko Aradi**[1], **Niklas Thon**[1], **Mariam Eghbal-Ahmadi**[1,2], **Tallie Z. Baram**[1,2], and **Ivan SoltesZ**[1]

[1]Department of Anatomy and Neurobiology, University of California at Irvine, Irvine, California, USA

[2]Department of Pediatrics, University of California at Irvine, Irvine, California, USA

Abstract

Febrile seizures are the most common type of developmental seizures, affecting up to 5% of children. Experimental complex febrile seizures involving the immature rat hippocampus led to a persistent lowering of seizure threshold despite an upregulation of inhibition. Here we provide a mechanistic resolution to this paradox by showing that, in the hippocampus of rats that had febrile seizures, the long-lasting enhancement of the widely expressed intrinsic membrane conductance I_h converts the potentiated synaptic inhibition to hyperexcitability in a frequency-dependent manner. The altered gain of this molecular inhibition–excitation converter reveals a new mechanism for controlling the balance of excitation–inhibition in the limbic system. In addition, here we show for the first time that h-channels are modified in a human neurological disease paradigm.

Puzzling increases of GABA (γ-aminobutyric acid)-mediated inhibition in hippocampus have been reported in several animal models of epilepsy[1–5]. However, the nature of the relationship between increased susceptibility for seizures and upregulated inhibition is not understood[6]. Could the enhancement of inhibition actually promote convulsions? Or, is the increase in inhibitory postsynaptic potentials (IPSPs) counteracted by pro-excitatory changes resulting from the seizures? These questions are particularly apt in the context of febrile seizures, which are the most common form of childhood seizures[7,8]. Using a novel rat model of complex febrile seizures[9,10], we have previously shown that prolonged hyperthermia-induced seizures at postnatal day 10 (P10) lead to a persistent increase in perisomatic inhibition of CA1 pyramidal neurons in the rat hippocampus[5]. Importantly, this increased inhibition was associated with a persistent decrease of seizure threshold[9]. For humans, a clinical association of complex febrile seizures with altered seizure threshold and development of temporal lobe epilepsy later in life has been put forth, but the precise mechanisms involved have been intensely debated[6–9,11].

H-channels are present in both cardiac and neuronal tissues, and play important functional roles, including the generation of the pacemaker current in the heart and sleep rhythms in thalamo-cortical neuronal circuits[12–16]. These channels are activated by hyperpolarization (hence their name) and generate a depolarizing current (I_h)[17–20]. Here we show that a single episode of hyperthermia-induced seizures at P10 leads to a novel form of long-term alteration in the properties of the I_h. The results show that the modified I_h in the

Correspondence should be addressed to I.S.; isoltesz@uci.edu.

experimental rats antagonizes repetitive inhibitory inputs and can convert them to post-inhibitory rebound firing in CA1 pyramidal cells. These findings constitute the first evidence that h-channels are persistently modified in a neurological disease paradigm, and the data may also provide a resolution to the long-standing paradox of increased inhibition in epilepsy.

Long-lasting alteration of I_h

One week following experimental prolonged febrile seizures, the membrane potential for half-maximal activation (V_{50}) of I_h was significantly shifted towards the depolarizing direction by 3.3 mV in CA1 pyramidal cells (Fig. 1*a*; control, V_{50} = −89.8 ± 0.7 mV, n = 6; after hyperthermia-induced seizures (HT), V_{50} = −86.5 ± 0.4 mV, n = 6; there was no difference in k values of the Boltzmann fit; control, 8.9 ± 0.2; HT, 8.8 ± 0.2). The h-current was significantly larger in HT animals even at low levels of hyperpolarization (for example, at −70 mV: control, 11.8 ± 1.1 pA; HT, 16.7 ± 1.6 pA). A positive shift in I_h activation was present nine weeks after febrile seizures (Fig. 1*b*; shift, 5.9 mV; control, V_{50} = −91.0 ± 0.4 mV, n = 10; HT, V_{50} = −85.1 ± 0.5 mV, n = 7). The shift in the activation curve could also be observed when recording in the perforated patch clamp configuration using gramicidin (Fig. 1*a*, lower left inset; control, V_{50} = −92.6 ± 0.5 mV, n = 4; HT, V_{50} = −86.7 ± 1.5 mV, n = 4). These data are the first demonstration of a persistent change in the properties of I_h.

The depolarizing shift in I_h activation was accompanied by an increase in both the fast and the slow time constants for activation (Fig. 2*a–c*; control, n = 16; HT, n = 18) one week after the induction of experimental febrile seizures. The slower kinetics of activation could be observed nine weeks after the induction of seizures (Fig. 2*b*, inset; control, n = 10; HT, n = 7). The relative weights of the fast and slow exponential fits did not change after the seizures (Fig. 1*c*, inset). The deactivation kinetics of I_h were also slower in the experimental animals (Fig. 2*d*; control, n = 9; HT, n = 11).

What could be the mechanism underlying the observed changes in the properties of I_h? In agreement with previous data[18], increased intracellular cAMP (cyclic adenosine monophosphate) levels (50 μM and 1 mM cAMP in the pipette) caused only a small, 1–2 mV depolarizing shift in the I_h activation curve in control cells (V_{50} measurements in controls: with 0 $cAMP_i$ = −89.8 ± 0.7 mV, n = 6; with 50 μM $cAMP_i$ = −89.3 ± 0.5 mV, n = 4; with 1 mM $cAMP_i$ = −88.3 ± 0.8 mV, n = 5). In cells from HT animals, 50 μM and 1 mM cAMP in the recording pipette also induced only small depolarizing shifts in the V_{50} (V_{50} measurements in HT: with 0 $cAMP_i$ = −86.5 ± 0.4 mV, n = 6; with 50 μM $cAMP_i$ = −85.6 ± 0.3 mV, n = 4; with 1 mM $cAMP_i$ = −85.6 ± 0.6, n = 5; Fig. 2*e*). The significant difference between the V_{50} measurements of I_h in cells from control versus HT animals was present even at the highest cAMP concentration.

The enhanced I_h was not due to persistent activation of protein kinase A (PKA), as the specific PKA inhibitor Rp-cAMPS (100 μM) did not abolish the difference between the activation curves (Fig. 2*f*; control, V_{50} = −91.7 ± 0.5 mV, n = 9; HT, V_{50}= −87.3 ± 0.6 mV, n = 6; 100 μM Rp-cAMPs under the same conditions blocked the enhancement of the inhibitory post synaptic currents (IPSCs) after febrile seizures[5]). Moreover, the shift in the activation curve could also be observed in the presence of the β-receptor antagonist propranolol[5] (1 μM; Fig. 2*f*, inset; V_{50} in control, −91.7 ± 0.5 mV; in HT, −87.9 ± 0.6 mV).

Interaction of inhibitory inputs and the modified I_h

Gramicidin-perforated patch clamp recordings revealed that cells from HT animals showed depolarized resting membrane potential (V_m; control, −61.0 ± 1.0 mV, n = 7; HT, −54.4 ± 2.5 mV, n = 7) and decreased input resistance (R_N; measured with small [< 10 mV]

hyperpolarizing pulses; control, 131.2 ± 8.4 MΩ, $n = 7$; HT, 103.5 ± 3.9 MΩ, $n = 7$; the R_N values were corrected for a drop in voltage across the series resistance, see Methods; these recordings were done in the presence of the $GABA_A$ channel blocker picrotoxin 100 μM, with the CA3-CA1 connection cut). Whole-cell recordings indicated that the selective h-channel blocker ZD-7288 (100 μM)[16,21] caused a larger hyperpolarization of V_m in cells from HT animals (control, 4.0 ± 1.0 mV, $n = 6$; HT, 7.3 ± 0.7mV, $n = 8$). These results are consistent with a more active I_h in cells from experimental animals even at potentials close to rest (Fig. 1).

The enhanced I_h opposed intracellularly evoked hyperpolarizations to a larger extent, resulting in a significantly greater depolarizing 'sag' in HT animals (Fig. 3*a* and *b*; control, $n = 4$; HT, $n = 4$). At the end of the current pulse, the larger, more slowly de-activating I_h in cells from HT animals led to a larger rebound depolarization (Fig. 3*a* and *b*). This rebound depolarization could evoke action potential discharges, which were blocked by ZD-7288 (Fig. 3*c*). Similar results were achieved when single or short trains of perisomatic IPSPs were elicited in the presence of the glutamate receptor antagonists APV (10 μM) and CNQX (5 μM), and the $GABA_B$ receptor antagonist SCH50911 (50 μM). Single IPSPs did not evoke rebound depolarization or firing in either control or experimental animals (Fig. 3*d*, inset). A short train of IPSPs (6 IPSPs at 50 Hz; similar IPSP trains occur spontaneously during θ rhythm *in vivo*[22]) rarely led to rebound firing in control cells. In contrast, a train of IPSPs triggered post-inhibitory rebound depolarization and firing in cells from HT rats (Fig. 3*d* and *e*; control, $n = 7$; HT, $n = 7$; there is no change in the threshold for action potential generation[5]; the reversal potential for IPSCs is also unaltered: control, −58.2 ± 1.7 mV, $n = 6$; HT, −60.1 ± 1.6 mV, $n = 7$). The post-inhibitory rebound depolarization and firing were abolished by ZD-7288 (Fig. 3*f*; $n = 5$). The blockade of the post-IPSP depolarization and firing by ZD-7288 in HT cells was not due to a presynaptic blocking effect, since the IPSPs were increased in amplitude in the presence of ZD-7288 (consistent with an increase in R_N following the blockade of h-channels; IPSP amplitude in ZD-7288, compared to the pre-ZD amplitude in the same HT cells: 125.1 ± 5.9%; see traces in Fig. 3*f*). In addition, intracellularly applied ZD-7288 (100 μM, included in the pipette solution[23]) blocked both the depolarizing sag and the post-IPSP rebound depolarization and firing in HT cells (Fig. 4*a*; $n = 4$), indicating that blockade of the postsynaptic h-channels alone is sufficient to inhibit the rebound firing. When the burst of evoked IPSPs was made depolarizing as a result of recording with Cl^- filled pipettes, no post-IPSP depolarization could be observed in HT cells (Fig. 4*b*; $n = 3$).

The post-IPSP rebound depolarization and firing in HT cells were not related to the bicarbonate-dependent, biphasic GABA response[24]. The stimulation frequency used in the previous experiments (6 stimuli at 50Hz) was too low to evoke the biphasic response in control cells (Fig. 3*d*). However, tetanic stimulation (40 stimuli at 100 Hz) evoked the biphasic hyperpolarization–depolarization sequence[24] in control cells (data not shown), which was blocked by recording in bicarbonate-free HEPES-buffered medium (Fig. 4*c*; $n = 3$). In contrast, CA1 cells from HT animals showed post-inhibitory rebound depolarization and firing in HEPES (Fig. 4*c*; $n = 3$). Also, the post-IPSP firing in HEPES in HT cells could be seen even with 6 stimuli at 50 Hz. Similar results were obtained when the biphasic response was blocked by the carbonic anhydrase blocker acetazolamide[24] (10 μM; Fig. 4*d*; control, $n = 3$; HT, $n = 5$).

Two potassium currents known to play important roles in neuronal excitability, the slowly inactivating K-current I_D (ref. 25) and the current underlying the slow after-hyperpolarization I_{AHP} (ref. 26), were identical in cells from HT and control animals (Fig. 4*e* and *f*; I_D, $n = 6$ for both control and HT; I_{AHP}, $n = 6$ for both groups). Moreover, there was no difference between the dendritic arborization of pyramidal cells in control and HT

animals (the relative number of equidistant apical dendritic segments of HT cells crossing the perimeters of concentric circles centered on the soma: middle layer: 107.1 ± 28.2%; outer layer: 100.0 ± 18.5%; $n = 5$ biocytin-filled cells in both groups). The lack of change in cell size was supported by the similar cell capacitance (for cells in Fig. 1*a*: control, 24.3 ± 0.7 pF; HT, 23.6 ± 0.9 pF). Additional experiments showed that spontaneous IPSCs (sIPSCs) recorded in control artificial cerebro-spinal fluid (ACSF) occurred in significantly larger, longer and more frequent bursts in CA1 cells from HT animals, indicating that the conditions for the activation of I_h by the inhibitory events exist in the animals which experienced seizures (Figs. 4*g* and *h*; control, $n = 22$; HT, $n = 28$).

Computational analysis of altered I_h and IPSPs

In order to study the alterations in I_h when all other factors can be kept constant, we constructed multicompartmental computer models of CA1 pyramidal cells[27,28]. 'HT' model cells were identical to control model cells, except in the shifted V_{50} and the slower kinetics of I_h (see Methods).

Single IPSPs, in either 'HT' or control model cells, did not significantly activate I_h or evoke rebound firing (Fig. 5*a*). In contrast, trains of IPSPs could evoke rebound firing, provided that the shift in I_h was more than 2 mV (Fig. 5*b*). When short trains of $GABA_A$ IPSPs were applied to the control model cells (shift in $I_h = 0$ mV), no rebound firing was elicited even when the IPSP amplitude was increased (Fig. 5*b*, traces labeled 'Control'). In contrast, in 'HT' model cells, the train of IPSPs evoked rebound depolarization, which, when the IPSP amplitude was increased, resulted in rebound firing (Fig. 5*b*). In addition, when a short train of inhibitory synaptic currents was applied, the amplitude of the IPSPs towards the end of the train was decreased to a larger extent in the 'HT' model cells compared to controls (data not shown).

The number of spikes following an IPSP train was enhanced when the density of the altered (that is, activation curve-shifted) h-channels was increased (data not shown). Experimentally, more rebound firing was observed following evoked IPSPs than following hyperpolarizing current steps (Fig. 3*b* and *d*). Stimulation near the cell layer is expected to activate mostly axo-axonic and basket-cell axons. However, since basket cells form synapses not only on the soma, but also on the proximal dendrites[29], it is likely that proximal dendritic h-channels were also directly (that is, locally) activated by the hyperpolarization caused by the IPSPs, whereas current injections supplied a current source confined to the soma. The density of h-channels linearly increases towards the distal dendrites both in real cells[30] and in our model cells. Activation of inhibitory synapses on the initial segment, soma and proximal dendrites ('perisomatic' inputs) resulted in more rebound firing than activation of inhibitory inputs confined to the soma ('somatic' inputs; in the latter case, the perisomatic synapses were moved to the soma; Fig. 5*c* and *d*). Similar results were obtained when hyperpolarizing current steps (instead of IPSPs) were used (Fig. 5*c* and *d*).

More proximal placement of the h-channels alone, without a shift in the I_h activation curve, did not lead to post-inhibitory rebound depolarizations and firing (Fig. 5*e*). Simulations also demonstrated that the depolarizing shift in the activation curve for I_h, even without including the changes in activation and deactivation kinetics in the model, was sufficient to lead to rebound depolarization and firing (Fig. 5*f*), whereas the slower kinetics alone (without including the shift in I_h activation) were not sufficient (Fig. 5*g*). Inclusion of a 4 mV shift in I_h activation in the model (that is, conversion of a control to an 'HT' model cell) caused an 18.8% decrease in input resistance, closely reproducing the experimentally observed 23% difference in R_N between cells from control and HT animals. Control model cells did not

exhibit significant post-IPSP depolarization, irrespective of whether the input resistance was set to 100 MΩ or 130 MΩ (R_N values observed experimentally; Fig. 5*h*). Moreover, rebound firing could be obtained when the V_{50} of only the somatic, or only the dendritic h-channels was changed (data not shown). Together, these computational studies support the experimental results, indicating that, 1) the modified I_h can powerfully regulate the influence of inhibitory inputs on CA1 cells following complex febrile seizures and that, 2) the depolarizing shift in I_h activation indeed plays a primary role in this process.

Discussion

Experimental complex febrile seizures result in a persistent, PKA-dependent, presynaptic potentiation of perisomatic, $GABA_A$ receptor-mediated IPSCs in CA1 pyramidal cells[5], and our data demonstrate that they can persistently modify intrinsic currents as well. Therefore, our results support the general conclusion of our previous studies[5,9], that prolonged hyperthermia-induced seizures cause long-lasting changes in neuronal excitability in the limbic system[6,31,32].

The molecular basis of I_h has been recently revealed through the cloning of the h-channels[18,20,33–35]. In CA1 pyramidal cells, HCN1 transcripts are in high abundance, however these cells express HCN2 as well (the latter form is predominant in the thalamus)[18,33–36]. HCN1 gene products are much less sensitive to cAMP modulation than HCN2 (typical shift in V_{50} in response to cAMP: HCN1, 2 mV; HCN2, 26 mV)[18,33–35]. In addition, HCN1 shows time constants of activation in the tens of milliseconds range, compared to hundreds of milliseconds for HCN2 (refs. 18,33–35). In general agreement with these expression studies, hippocampal CA1 cells show a more hyperpolarized V_{50}, faster kinetics and only a small positive shift following cAMP rises, compared with thalamic projection neurons[14,18,33,37,38].

A positive shift in I_h activation is thought to be associated with increased cAMP levels[17,18]. It is not known whether cAMP levels are persistently increased after seizures. However, the fact that we could not abolish the difference in V_{50} measurements by recording with pipettes containing high cAMP concentrations indicates that simple increases in cAMP levels are unlikely to fully explain the observed shift in I_h activation. In addition, increased cAMP levels should result in acceleration of activation kinetics[17,18,20], whereas I_h activation was slower after hyperthermia-induced seizures. The slower kinetics of I_h is compatible with a possible relative increase in HCN2 expression; however, inclusion of cAMP in the recording pipette did not cause a larger shift in HT cells than in controls. Although the action of cAMP on h-channels is thought to be direct and not mediated through the PKA pathway[39], it is still noteworthy that our results showed that increased PKA activity is unlikely to underlie the long-term shift in I_h following the seizures, especially since the upregulation of inhibition following hyperthermia-induced seizures was abolished by PKA-blockade[5]. Our data show that the activation and de-activation of I_h can be described by double exponentials in both HT and control animals. But it is unclear whether the double exponential behavior reflects distinct fast and slow channels in the same cells, or a complex activation path for a single channel population[16–18,40]. However, both the fast and the slow time constants appeared to undergo modifications following hyperthermia-induced seizures. Although the exact molecular mechanism underlying the observed changes in I_h following complex febrile seizures is not fully elucidated, these changes constitute the first demonstration of the involvement of I_h in clinically relevant brain pathology. In addition, these data are the first evidence for long-term (weeks and months) modification of h-channels in the central nervous system. Our data on I_h also raise the possibility that other hyperpolarization-activated, inwardly rectifying conductances[41] expressed in CA1 may also undergo long-term modulation following seizures during development.

As increased inhibitory currents have been described in several models of epilepsy[1–5], the question of the role of the potentiated inhibition (that is, is it pro- or anti-convulsive?) in the context of a hyperexcitable brain becomes especially important[6]. Our recent results indicated that rats that experienced hyperthermia-induced seizures at P10 did not exhibit spontaneous electrographic or behavioral seizures as adults[9]. However, these animals had a lowered seizure threshold when challenged with either kainic acid *in vivo* or tetanic stimulation *in vitro*[9]. Our data indicate that when IPSPs occur at high frequencies and summate, they activate I_h particularly well in the HT animals (since the inhibitory inputs are potentiated and I_h is positively shifted in its activation). The activated I_h, in turn, opposes the IPSPs and can result in pyramidal-cell discharges following the inhibitory barrage. Thus, the altered gain of I_h effectively neutralizes the seizure-induced enhancement of IPSPs, since the larger and more frequent the incoming hyperpolarizing inputs become, the more I_h will be activated. Therefore, whether increased inhibition after febrile seizures[5] is inhibitory or excitatory depends on the temporal structure of the IPSPs: single IPSPs do not activate I_h and do not lead to rebound firing, whereas bursts of higher-frequency IPSPs can do so. Although our findings can provide a solution to the 'increased inhibition paradox' of epilepsy[6], there may be other mechanisms which can limit the effects of potentiated IPSPs in epilepsy in general[4,24], and following febrile seizures in particular, in addition to enhanced I_h.

In conclusion, these results implicate I_h as a mechanistic component of a central nervous system disorder, and demonstrate that the long-term enhancement of I_h contributes to a frequency-dependent collapse of potentiated inhibition in animals that experienced febrile seizures during development. The future development of subtype-selective h-channel antagonists may provide effective tools for controlling the interaction of inhibition and intrinsic membrane currents in epilepsy.

Methods

Slice preparation

Control and experimental littermate Sprague-Dawley rats (Zivic-Miller, Zelienople, Pennsylvania) were killed 1–9 wk after complex febrile seizures and the brains were removed. Brain slices were prepared[5] in ACSF consisting of (in mM): 126 NaCl, 2.5 KCl, 26 $NaHCO_3$, 2 $CaCl_2$, 2 $MgCl_2$, 1.25 NaH_2PO_4 and 10 glucose.

Electrophysiology

Blind whole-cell recordings were obtained in an interface-type chamber at 35 °C, using Axopatch-200A amplifier (Axon Instruments, Foster City, California). IPSPs were recorded in ACSF containing 10 μM 2-amino-5-phosphovaleric acid (APV; Tocris, Ballwin, Missouri), 5 μM 6-cyano-7-nitroquinoxaline-2,3-dione (CNQX; Tocris) and 50 μM SCH50911 (Tocris). For I_h, the ACSF contained 10 μM APV, 5 μM CNQX, 1 μM tetrodotoxin (TTX; Calbiochem, La Jolla, California), 10 mM tetraethylammonium (TEA, Sigma), 0.5 mM 4-aminopyridine (4-AP; Research Biochemicals International; RBI), 0.1 mM $CdCl_2$ (Sigma), 1 mM $BaCl_2$ (Sigma), and 10 μM bicuculline (RBI). To evoke perisomatic IPSPs (latency, < 3.1 ms), constant-current stimuli (20 μs) were applied through a bipolar 90 μm tungsten electrode. The placement and distance of the recording and stimulating electrodes were kept constant as described[5]. Pipette solutions consisted of (in mM) 140 K-gluconate, 2 $MgCl_2$, 10 N-2-hydroxyethylpiperazine-N-2-ethanesulfonic acid (HEPES), and, when indicated, cAMP (Sigma). I_D (ref. 25) was recorded by subtracting current recorded in 40μM 4-aminopyridin (4-AP) from pre–4-AP recordings. For I_{AHP} (ref. 26), neurons were voltage clamped at −60 mV, and 100 ms depolarizing pulses to −20 mV were delivered to evoke Ca^{++}-currents; I_{AHP} was sensitive to carbachol[26] (2.5 μM; $n = 4$).

For nominally bicarbonate-free medium, $NaHCO_3$ was omitted, HEPES was added[24], and the medium was gassed with 100% O_2. Spontaneous IPSCs were recorded at 0 mV with Cs-gluconate-containing pipettes (sIPSC bursts: > 400 pA events lasting > 150 ms; burst ended when current was < 80 pA for > 10 ms).

Analysis

Recordings were filtered at 3 kHz before digitization at 20 kHz using Strathclyde Electrophysiology Software (from J. Dempster) and Synapse software (from Y. De Koninck). I_h data were fitted with the Boltzmann equation. To assess whether the rise or decay of I_h was better fitted with single versus double exponentials, the 'SSE Improvement' function[42] was used. Briefly, F-test assessed the improvement in the ratio $SSE_1 - SSE_2/SSE_2$ where SSE_1 and SSE_2 are sum of squared errors of fits with 1 and 2 exponentials, respectively; when 'SSE improvement' is not significant, the current can be described by single exponential[42]. For R_N from gramicidin-recordings, the membrane potential values were corrected for voltage-drop across series resistance: $V_{corr} = V_{com} - I_{clamp} \times R_S$, where V_{com} is command potential, I_{clamp} is clamp current, and R_S is series resistance. Statistical analyses (for measurements other than the 'SSE Improvement', a *t*-test) was performed with SigmaPlot or SPSS, with a level of significance of $P < 0.05$. Data are presented as mean ± s.e., and '*n*' is the number of recorded cells.

Computer modeling

Multicompartmental models of CA1 pyramidal cells were constructed with the NEURON software[27], using compartments for the soma (2 compartments, 20 μm length, 20 μm diameter), proximal, middle, distal apical dendrites (each with 2 compartments, 150 μm length, 2 μm diameter), basal dendrites (2 compartments, 200 μm length, 2 μm diameter) and axon (2 compartments, 100 μm length, 0.5 μm diameter). Passive parameters (R_N, 100 MΩ or 130 MΩ; membrane time constant, 25 ms) were obtained from experimental data, in agreement with published values[5,43]. Model cells included sodium-, delayed rectifier potassium- and h-currents. The equations for sodium and potassium channel kinetics were from a hippocampal granule cell model[28] describing similar channel kinetics found in pyramidal cells[44,45]. The experimentally determined I_h activation and kinetics were fitted and used in the simulations. The model simulated the non-homogeneous h-channel distribution[30], that is, a seven-fold linear increase in channel density from the somatic (density, 0.15 mS/cm^2) to the most distal dendritic compartment (1.05 mS/cm^2). Moreover, as found experimentally[30], the V_{50} of I_h in the somatic compartment was 10 mV more depolarized compared with the most distal compartment, and linearly shifted in between. 'HT' model cells differed from controls only in, 1) the positively shifted V_{50} of I_h activation in each of the corresponding compartments and, 2) in the slower activation and deactivation kinetics. The perisomatic IPSPs were modeled using exponential functions reproducing the amplitude and kinetics measured experimentally[5]. For further details, see http://www.ucihs.uci.edu/anatomy/soltesz/supp.htm.

Hyperthermia-induced seizures

The hyperthermia-induced seizure paradigm has been described[5,9,10]. Briefly, on P10, the core temperature of pups was raised using a regulated stream of moderately heated air. Hyperthermia (defined as a core temperature greater than 39.5 °C) was maintained for 30 min. Seizure duration in this model has been shown to average 22.8 ± 0.3 min, and threshold temperature to seizure onset averaged 41.1 °C (refs. 5,9). Following the hyperthermia period, rats were placed on a cool surface, monitored for 15 min, and then returned to home cages. The behavioral seizures in this paradigm are stereotyped and correlate with EEG rhythmic epileptiform discharges from the hippocampus and amygdala[9,10].

Acknowledgments

We thank R. Zhu for technical assistance. This work was financially supported by the NIH (NS38580 to I.S. and NS35439 to T.Z.B.), by the UC Systemwide Biotechnology Research and Education Program (BREP-98-02 to T.Z.B. & I.S.) and by a Postdoctoral Fellowship from the Epilepsy Foundation of America (to I.A.).

References

1. Otis TS, De Koninck Y, Mody I. Lasting potentiation of inhibition is associated with an increased number of gamma-aminobutyric acid type A receptors activated during miniature inhibitory postsynaptic currents. Proc Natl Acad Sci USA. 1994; 91:7698–702. [PubMed: 8052645]
2. Nusser Z, Hájos N, Somogyi P, Mody I. Increased number of synaptic GABA(A) receptors underlies potentiation at hippocampal inhibitory synapses. Nature. 1998; 395:172–177. [PubMed: 9744275]
3. Brooks-Kayal AR, Shumate MD, Jin H, Rikhter TY, Coulter DA. Selective changes in single cell $GABA_A$ receptor subunit expression and function in temporal lobe epilepsy. Nature Med. 1998; 4:1166–1172. [PubMed: 9771750]
4. Buhl EH, Otis TS, Mody I. Zinc-induced collapse of augmented inhibition by GABA in a temporal lobe epilepsy model. Science. 1996; 271:369–373. [PubMed: 8553076]
5. Chen K, Baram TZ, Soltesz I. Febrile seizures in the developing brain result in persistent modification of neuronal excitability in limbic circuits. Nature Med. 1999; 5:888–894. [PubMed: 10426311]
6. Walker MC, Kullmann DM. Febrile convulsions: a 'benign' condition? Nature Med. 1999; 5:871–872. [PubMed: 10426304]
7. Shinnar S. Prolonged febrile seizures and mesial temporal sclerosis. Ann Neurol. 1998; 43:411–412. [PubMed: 9546320]
8. Cendes F, et al. Early childhood prolonged febrile convulsions, atrophy and sclerosis of mesial structures, and temporal lobe epilepsy: an MRI volumetric study. Neurology. 1993; 43:1083–1087. [PubMed: 8170546]
9. Dube C, et al. Prolonged febrile seizures in the immature rat model enhance hippocampal excitability long term. Ann Neurol. 2000; 47:336–344. [PubMed: 10716253]
10. Baram TZ, Gerth A, Schultz L. Febrile seizures: an appropriate-aged model suitable for long-term studies. Dev Brain Res. 1997; 98:265–270. [PubMed: 9051269]
11. VanLandingham KE, Heinz ER, Cavazos JE, Lewis DV. Magnetic resonance imaging evidence of hippocampal injury after prolonged focal febrile convulsions. Ann Neurol. 1998; 43:413–426. [PubMed: 9546321]
12. Brown HF, DiFrancesco D, Noble SJ. How does adrenaline accelerate the heart? Nature. 1979; 280:235–236. [PubMed: 450140]
13. Mayer ML, Westbrook GL. A voltage-clamp analysis of inward (anomalous) rectification in mouse spinal sensory ganglion neurones. J Physiol (Lond). 1983; 340:19–45. [PubMed: 6887047]
14. Pape HC, McCormick DA. Noradrenaline and serotonin selectively modulate thalamic burst firing by enhancing a hyperpolarization-activated cation current. Nature. 1989; 340:715–718. [PubMed: 2475782]
15. Soltesz I, et al. Two inward currents and the transformation of low-frequency oscillations of thalamocortical cells. J Physiol (Lond). 1991; 441:175–197. [PubMed: 1667794]
16. Maccaferri G, McBain CJ. The hyperpolarization-activated current (I_h) and its contribution to pacemaker activity in rat CA1 hippocampal stratum oriens-alveus interneurones. J Physiol (Lond). 1996; 497:119–130. [PubMed: 8951716]
17. Pape HC. Queer current and pacemaker: the hyperpolarization-activated cation current in neurons. Ann Rev Physiol. 1996; 58:299–327. [PubMed: 8815797]
18. Santoro B, Tibbs GR. The HCN gene family: molecular basis of the hyperpolarization-activated pacemaker channels. Ann NY Acad Sci. 1999; 868:741–764. [PubMed: 10414361]
19. Beaumont V, Zucker RS. Enhancement of synaptic transmission by cyclic AMP modulation of presynaptic I_h channels. Nature Neurosci. 2000; 3:133–141. [PubMed: 10649568]

20. Siegelbaum SA. Presynaptic facilitation by hyperpolarization-activated pacemaker channels. Nature Neurosci. 2000; 3:101–102. [PubMed: 10649561]
21. BoSmith RE, Briggs I, Sturgess NC. Inhibitory actions of ZENECA ZD7288 on whole-cell hyperpolarization activated inward current (I_f) in guinea-pig dissociated sinoatrial node cells. Brit J Pharm. 1993; 110:343–349.
22. Soltesz I, Deschênes M. Low- and high-frequency membrane-potential oscillations during theta activity in morphologically identified neurons of the rat hippocampus during ketamine-xylazine anesthesia. J Neurophysiol. 1993; 70:97–116. [PubMed: 8395591]
23. Harris NC, Constanti A. Mechanism of block by ZD-7288 of the hyperpolarization-activated inward rectifying current in guinea pig substantia nigra neurons in vitro. J Neurophysiol. 1995; 74:2366–2378. [PubMed: 8747199]
24. Staley KJ, Soldo BL, Proctor WR. Ionic mechanisms of neuronal excitation by inhibitory $GABA_A$ receptors. Science. 1995; 269:977–981. [PubMed: 7638623]
25. Storm JF. Temporal integration by a slowly inactivating K^+ current in hippocampal neurons. Nature. 1988; 336:379–381. [PubMed: 3194020]
26. Krause M, Pedarzani P. A protein phosphatase is involved in the cholinergic suppression of the Ca^{2+}-activated K^+ current sI_{AHP} in hippocampal pyramidal neurons. Neuropharmacology. 2000; 39:1274–1283. [PubMed: 10760369]
27. Hines, ML. Computer modeling methods for neurons. In: Arbib, MA., editor. The Handbook of Brain Theory and Neural Networks. MIT Press; Cambridge, Massachusetts: 1995. p. 226-230.
28. Aradi I, Holmes WR. Role of multiple calcium and calcium-dependent conductances in regulation of hippocampal dentate granule cell excitability. J Comput Neurosci. 1999; 6:215–235. [PubMed: 10406134]
29. Freund TF, Buzsáki G. Interneurons of the hippocampus. Hippocampus. 1996; 6:347–470. [PubMed: 8915675]
30. Magee JC. Dendritic hyperpolarization-activated currents modify the integrative properties of hippocampal CA1 pyramidal neurons. J Neurosci. 1998; 18:7613–7624. [PubMed: 9742133]
31. Holmes GL, Ben-Ari Y. Seizures in the developing brain: Perhaps not so benign after all. Neuron. 1998; 21:1231–1234. [PubMed: 9883716]
32. Villeneuve N, Ben-Ari Y, Holmes GL, Gaiarsa JL. Neonatal seizures induced persistent changes in intrinsic properties of CA1 rat hippocampal cells. Ann Neurol. 2000; 47:729–738. [PubMed: 10852538]
33. Santoro B, Grant SG, Bartsch D, Kandel ER. Interactive cloning with the SH3 domain of N-src identifies a new brain specific ion channel protein, with homology to eag and cyclic nucleotide-gated channels. Proc Natl Acad Sci USA. 1997; 94:14815–14820. [PubMed: 9405696]
34. Santoro B, et al. Identification of a gene encoding a hyperpolarization-activated pacemaker channel of brain. Cell. 1998; 93:717–729. [PubMed: 9630217]
35. Ludwig A, Zong X, Jeglitsch M, Hofmann F, Biel M. A family of hyperpolarization-activated mammalian cation channels. Nature. 1998; 393:587–591. [PubMed: 9634236]
36. Moosmang S, Biel M, Hofmann F, Ludwig A. Differential distribution of four hyperpolarization-activated cation channels in mouse brain. Biol Chem. 1999; 380:975–980. [PubMed: 10494850]
37. Maccaferri G, Mangoni M, Lazzari A, DiFrancesco D. Properties of the hyperpolarization-activated current in rat hippocampal CA1 pyramidal cells. J Neurophysiol. 1993; 69:2129–2136. [PubMed: 7688802]
38. Lüthi A, McCormick DA. Modulation of a pacemaker current through Ca^{2+}-induced stimulation of cAMP production. Nature Neurosci. 1999; 2:634–41. [PubMed: 10404196]
39. DiFrancesco D, Tortora P. Direct activation of cardiac pacemaker channels by intracellular cyclic AMP. Nature. 1991; 351:145–7. [PubMed: 1709448]
40. Baker K, Warren KS, Yellen G, Fishman MC. Defective “pacemaker” current (I_h) in a zebrafish mutant with a slow heart rate. Proc Natl Acad Sci USA. 1997; 94:4554–4559. [PubMed: 9114028]
41. Smith RL, Clayton GH, Wilcox CL, Escudero KW, Staley KJ. Differential expression of an inwardly rectifying chloride conductance in rat brain neurons: A potential mechanism for cell-specific modulation of inhibition. J Neurosci. 1995; 15:4057–4067. [PubMed: 7751965]

42. Hollrigel GH, Toth K, Soltesz I. Neuroprotection by propofol in acute mechanical injury: Role of GABAergic inhibition. J Neurophysiol. 1996; 76:2412–2422. [PubMed: 8899614]

43. Spruston N, Johnston D. Perforated patch-clamp analysis of the passive membrane properties of three classes of hippocampal neurons. J Neurophysiol. 1992; 67:508–529. [PubMed: 1578242]

44. Numann RE, Wadman WJ, Wong RK. Outward currents of single hippocampal cells obtained from the adult guinea-pig. J Physiol (Lond). 1987; 393:331–353. [PubMed: 2451740]

45. Magee JC, Johnston D. Characterization of single voltage-gated Na^+ and Ca^{2+} channels in apical dendrites of rat CA1 pyramidal neurons. J Physiol (Lond). 1995; 487:67–90. [PubMed: 7473260]

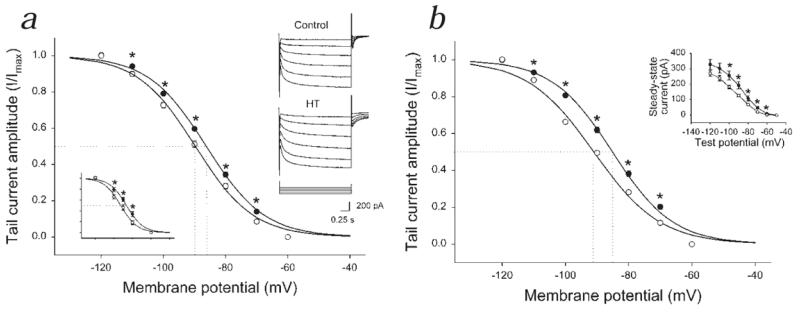

Fig 1.

Long-lasting shift in h-current activation following hyperthermia-induced seizures. ***a***, I_h activation in CA1 cells from animals one week after seizures (●) and sham-treated littermate controls (○). The fitted curve is the Boltzmann function. The data points are normalized per cell and averaged. R_S: control, 8.5 ± 1.1 MΩ; HT, 10.1 ± 1.7 MΩ; no difference. The maximal tail current did not increase; at −120 mV: control, 127.6 ± 8.6 pA; HT, 119.1 ± 8.7 pA. The tail current tended to saturate at negative voltages; currents at −120 mV and −110 mV were not statistically different in either group. Right inset, Raw traces; voltage stepped from −40 mV up to −120 mV, then to −60 mV. Left inset, Gramicidin recordings (1 wk post-seizure; R_S: control, 40.8 ± 4.6 MΩ; HT, 41.0 ± 3.4 MΩ; no difference). ***b***, I_h activation 9 wk after seizures (●) and in controls (○). R_S: control, 9.6 ± 1.0 MΩ; HT, 9.0 ± 1.0 MΩ; no difference). Inset, Steady-state current (following subtraction of instantaneous current; 9 wk after seizures).

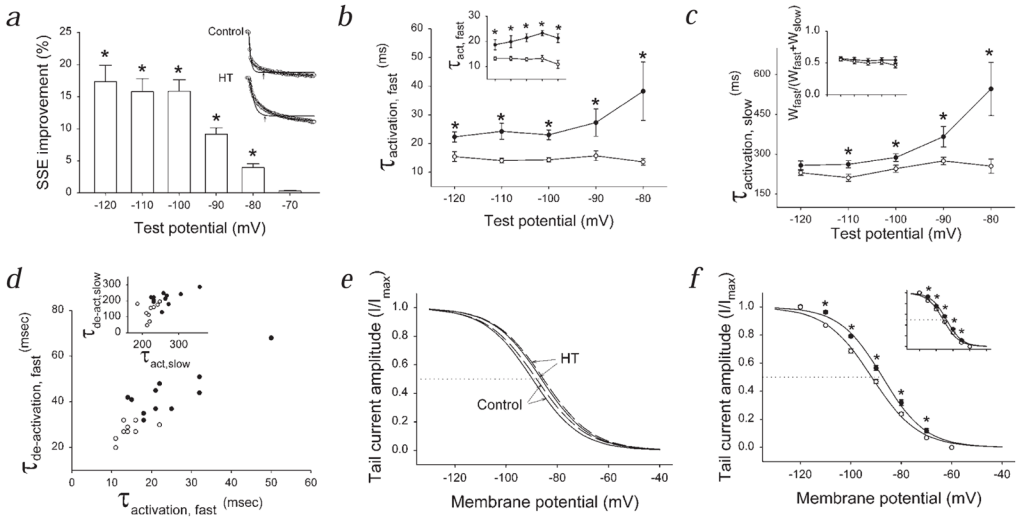

Fig. 2.

Kinetic changes in I_h following seizures and the effect of modulation of intracellular cAMP. ***a***, 'SSE Improvement' shows that double exponentials provided better fits to I_h at most voltages. *Inset*, Traces evoked at −110mV; single exponentials (arrows) provided poorer fits than double exponentials. ***b***, Voltage versus fast activation time constants (1 wk after seizures; in *b–f,* control, ○; HT, ●). *Inset*, Activation kinetics 9 wk following seizures. ***c***, Voltage versus slow activation time constants. *Inset*, Weights of fast and slow exponential components (w_{fast} and w_{slow}, respectively). ***d***, Fast activation versus fast de-activation rates (data points are mean values from cells at −110 mV). *Inset*, Slow activation and de-activation time constants. ***e***, I_h activation curves without (continuous lines) and with 1 mM cAMP (dashed lines) in the pipette. ***f***, I_h activation curves in Rp-cAMPS. *Inset*, Activation curves in propranolol.

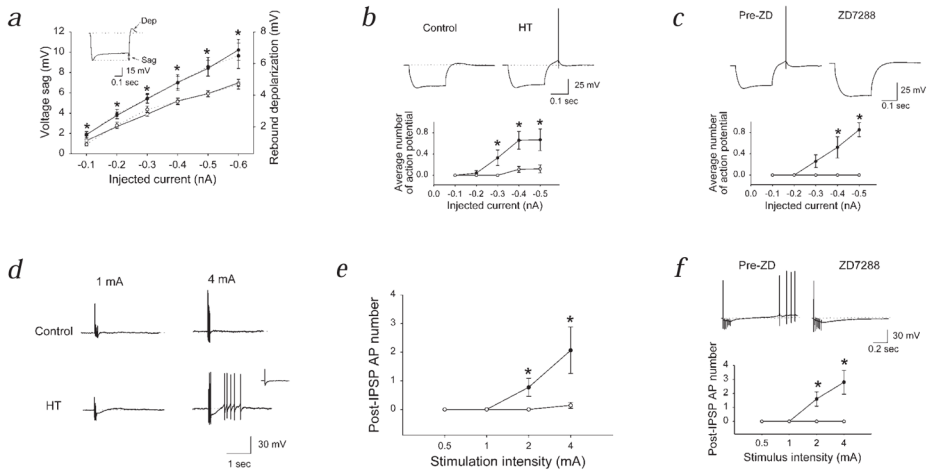

Fig. 3.

Enhanced activation of altered I_h by hyperpolarizing inputs and post-inhibitory rebound firing following hyperthermia-induced seizures. ***a***, Intracellularly injected hyperpolarizing current amplitude versus the depolarizing 'sag' (left y-axis; continuous lines), and the rebound depolarization 'dep'; right y-axis; dotted lines). In control ACSF, cells held at −60 mV to avoid rebound firing. ***b***, Rebound firing. Membrane potential: control, −54.1 ± 1.6 mV; HT, −53.3 ± 2.0 mV. In *b–f*, APV, CNQX and SCH50911 were present. ***c***, Block of rebound firing and depolarization by ZD-7288 in cells from HT animals (Pre-ZD, ●; ZD-7288, ○). ***d***, IPSPs (6 stimuli at 50Hz) and rebound firing in HT animals. *Inset*, Single IPSP. ***e***, Summary data for post-inhibitory firing from experiments similar to those in *d* (membrane potential: control, −53.3 ± 2.4 mV; HT, −53.4 ± 1.3 mV; the duration of the post-IPSP depolarization was also longer by 321.0 ± 67% in HT. ***f***, Block of post-inhibitory rebound firing by ZD-7288 in HT cells. Throughout this figure (except for c and f): control, ○; HT, ●.

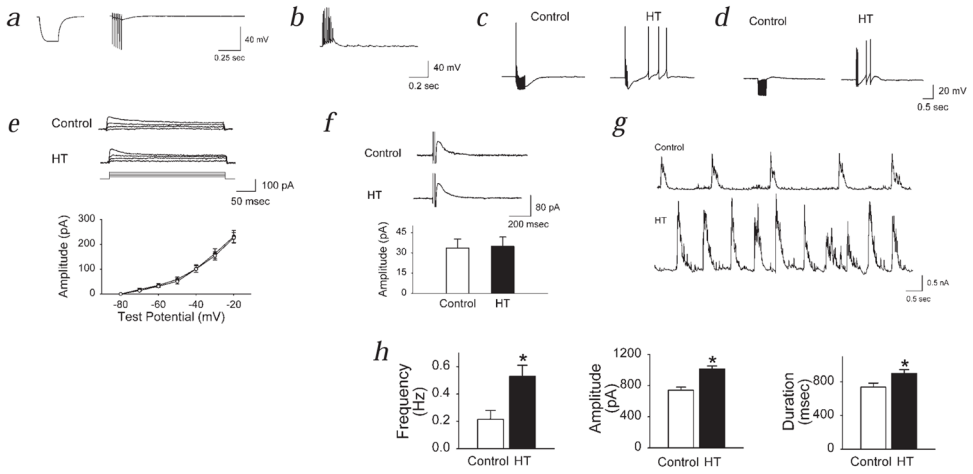

Fig. 4.

Mechanism of post-inhibitory rebound firing, specificity of the changes affecting I_h, and pattern of spontaneous GABA-receptor activation after febrile seizures. ***a***, Block of the sag response and the post-IPSP firing following intracellular application of ZD-7288 (stimulation: as in Fig. 3; hyperpolarization of V_m by extracellular ZD-7288 with intracellular ZD-7288 present, 0.5 ± 0.5 mV, $n = 4$; without intracellular ZD-7288, 7.3 ± 0.7, $n = 8$). ***b***, Evoked IPSPs with Cl^- filled pipettes ($E_{Cl} = 0$ mV). ***c*** and ***d***, Rebound firing in HEPES/O_2 buffer (*c*) and in acetazolamide (*d*). Control, 40 stimuli at 100 Hz; HT, 6 stimuli at 50 Hz. ***e*** and ***f***, Lack of a change in I_D (*e,* control, ○; HT, ●) and I_{AHP} (*f*) after seizures. ***g*** and ***h***, Spontaneous IPSCs after experimental febrile seizures (intra-burst IPSC frequency: 95.1 ± 10.6 Hz).

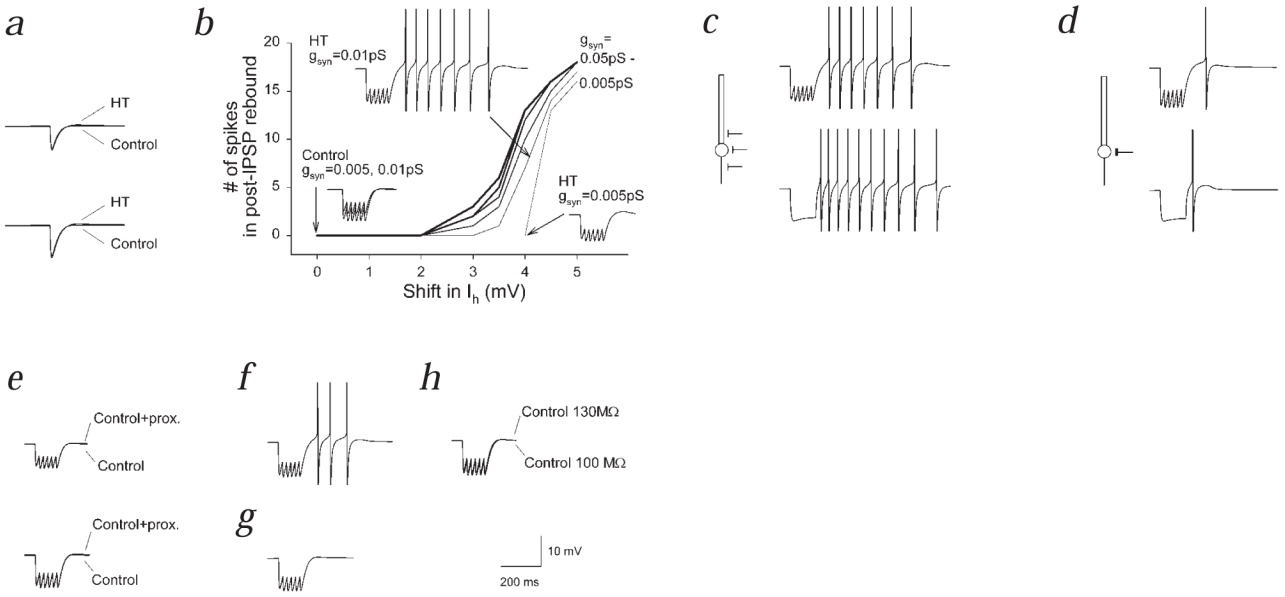

Fig. 5.

Multicompartmental modeling shows importance of altered h-channels in limiting inhibitory inputs and generating post-inhibitory rebound firing. ***a***, Single IPSPs, of smaller (upper panel) or larger amplitude (lower panel), did not result in rebound firing. ***b***, Dependence of rebound firing on shift in I_h and on the strength of inhibition (g_{syn}). ***c*** and ***d***, Dependence of post-inhibitory rebound firing on the position of inhibitory inputs along the somatodendritic axis (*c*, 'perisomatic' inputs; *d*, 'somatic' inputs; upper panels, inhibitory synaptic inputs; lower panels, hyperpolarizing current steps). ***e***, Lack of significant rebound firing following placement of all dendritic h-channels into the most proximal dendritic compartment; upper panel, small IPSPs; lower panel, larger IPSPs. ***f***, Shifted V_{50} for I_h, but I_h kinetics were kept control-like. ***g***, No shift in V_{50}, but HT-like kinetics. ***h***, Lack of rebound firing when input resistance was decreased (as found experimentally after seizures) in a control model cell.